

ResIST: Layer-Wise Decomposition of ResNets for Distributed Training

Chen Dun*

cd46@rice.edu

Department of Computer Science, Rice University
Houston, Texas, USA

Christopher M. Jermaine

Christopher.M.Jermaine@rice.edu

Department of Computer Science, Rice University
Houston, Texas, USA

Cameron R. Wolfe*

crw13@rice.edu

Department of Computer Science, Rice University
Houston, Texas, USA

Anastasios Kyrellidis

anastasios@rice.edu

Department of Computer Science, Rice University
Houston, Texas, USA

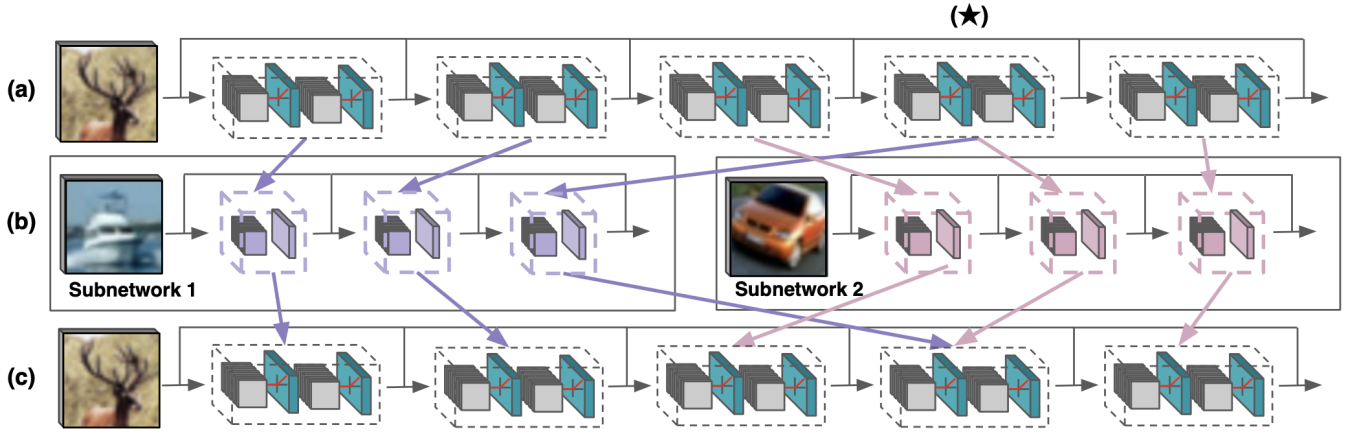


Figure 1: The ResIST model: we depict the process of partitioning the layers of a ResNet to different sub-ResNets, then aggregating the updated parameters back into the global network. Row (a) represents the original global ResNet. Row (b) shows the creation of two sub-ResNets. Observe that subnetwork 1 contains the residual blocks #1, #2 and #4, while subnetwork 2 contains the residual blocks #3, #4 and #5. Row (c) shows the reassembly of the global ResNet, after locally training subnetworks 1 and 2 for some number of local SGD iterations; residual blocks that are common across subnetworks (e.g., residual block #4, marked with a ★) are aggregated appropriately during the reassembly.

ABSTRACT

We propose ResIST, a novel distributed training protocol for Residual Networks (ResNets). ResIST randomly decomposes a global ResNet into several shallow sub-ResNets that are trained independently in a distributed manner for several local iterations, before having their updates synchronized and aggregated into the global model. In the next round, new sub-ResNets are randomly generated and the process repeats. By construction, per iteration, ResIST communicates only a small portion of network parameters to each machine and never uses the full model during training. Thus, ResIST reduces the communication, memory, and time requirements of ResNet training to only a fraction of the requirements of previous methods. In comparison to common protocols like data-parallel training and data-parallel training with local SGD, ResIST yields a decrease in wall-clock training time, while being competitive with respect to model performance.

1 INTRODUCTION

Background. In recent years, the field of Computer Vision (CV) has seen a revolution, beginning with the introduction of AlexNet during the ILSVRC2012 competition [14, 38]. Following this initial application of deep convolutional neural networks (CNNs), more modern architectures were produced, thus rapidly pushing the state of the art in image recognition [58, 62, 81]. In particular, the introduction of the residual connection (ResNets) allowed these networks to be scaled to massive depths without being crippled by issues of unstable gradients during training [25]. Such ability to train large networks was only furthered by the development of architectural advancements, like batch normalization [29]. The capabilities of ResNets have been further expanded in recent years, but the basic ResNet architecture has remained widely-used [26, 71]. While ResNets have become a standard building block for the advancement of CV research [24, 27, 44, 54], the computational requirements for training them are significant. For example, training

*Both authors contributed equally to this research.

a ResNet50 on ImageNet with a single NVIDIA M40 GPU takes 14 days. [74]

Therefore, distributed training with multiple GPUs is commonly adopted to speed up the training process for ResNets. Yet, such acceleration is achieved at the cost of a remarkably large number of GPUs (e.g. 256 NVIDIA Tesla P100 GPU [21]). Additionally, frequent synchronization and high communication costs create bottlenecks that hinder such methods from achieving linear speedup with respect to the number of available GPUs [57, 65]. Asynchronous approaches avoid the cost of synchronization, but stale updates complicate their optimization process [5]. Other methods, such as data-parallel training with local SGD [9, 43, 60, 82], reduce the frequency of synchronization. Similarly, model-parallel training has gained in popularity by decreasing the cost of local training between synchronization rounds [8, 10, 19, 22, 23, 35, 51, 66, 84].

This paper. We focus on efficient distributed training of convolutional neural networks with residual skip connections. Our proposed methodology accelerates synchronous, distributed training by leveraging ResNet robustness to layer removal [28]. In particular, a group of high-performing subnetworks (sub-ResNets) is created by partitioning the layers of a shared ResNet model to create multiple, shallower sub-ResNets. These sub-ResNets are then trained independently (in parallel) for several iterations before aggregating their updates into the global model and beginning the next iteration. Through the local, independent training of shallow sub-ResNets, this methodology both limits synchronization and communicates fewer parameters per synchronization cycle, thus drastically reducing communication overhead. We name this scheme *ResNet Independent Subnetwork Training* (ResIST). The outcome of this work can be summarized as follows:

- We propose a distributed training scheme for ResNets, dubbed ResIST, that partitions the layers of a global model to multiple, shallow sub-ResNets, which are then trained independently between synchronization rounds.
- We perform extensive ablation experiments to motivate the design choices for ResIST, indicating that optimal performance is achieved by *i)* using pre-activation ResNets, *ii)* scaling intermediate activations of the global network at inference time, *iii)* sharing layers between sub-ResNets that are sensitive to pruning, and *iv)* imposing a minimum depth on sub-ResNets during training.
- ResIST is shown to achieve high accuracy and time efficiency in all cases. We conduct experiments on several image classification and object detection datasets, including CIFAR10/100, ImageNet, and PascalVOC.
- We utilize ResIST to train numerous different ResNet architectures (e.g., ResNet101, ResNet152, and ResNet200) and provide implementations for each in PyTorch [50].

2 INDEPENDENT SUB-RESNET TRAINING WITH RESNETS

ResIST operates by partitioning the layers of a global ResNet to different, shallower sub-ResNets, training those independently, and intermittently aggregating their updates into the global model. The high-level process followed by ResIST is depicted in Fig. 1 and outlined in more detail by Algorithm 1. *We note that a naive, uniform*

partitioning of blocks to each subnetwork, resembling a distributed implementation of [28], performs poorly (see Fig. 5). To improve upon this procedure, extensive experiments, outlined in Sec. 6.1, are conducted to motivate design choices of ResIST, leading to a final methodology that generalizes well across domains and datasets.

2.1 Model Architecture

To achieve optimal performance with ResIST, the global model must be sufficiently deep. Otherwise, sub-ResNets may become too shallow after partitioning, leading to poor performance. For most experiments, a ResNet101 architecture is selected, which balances sufficient depth with reasonable computational complexity. Experiments with deeper architectures are also provided in Sec. 6.4.

ResIST performs best with pre-activation ResNets [26]. Intuitively, applying batch normalization prior to the convolution ensures that the input distribution of remaining residual blocks will remain fixed, even when certain layers are removed from the architecture. The Pre-activation ResNet101, which we utilize for the majority of experiments, is depicted in Fig. 2. This model, as well as deeper variants (e.g., ResNet152 and ResNet200), are readily available through deep learning packages like PyTorch [50] and Tensorflow [1].

2.2 Sub-ResNet Construction

Pruning literature has shown that strided layers, initial layers, and final layers within CNNs are sensitive to pruning [39]. Additionally, repeated blocks of identical convolutions (i.e., equal channel size and spatial resolution) are less sensitive to pruning [39]. Drawing upon these results, ResIST only partitions blocks within the third section of the ResNet (see the highlighted section in Fig. 2), while all other blocks are shared between sub-ResNets. These blocks are chosen for partitioning because *i)* they account for the majority of network layers; *ii)* they are not strided; *iii)* they are located within the middle of the network (i.e., initial and final layers are excluded); and *iv)* they reside within a long chain of identical convolutions. By partitioning only these blocks, ResIST allows sub-ResNets to be shallower than the global network, while maintaining high performance.

The process of constructing sub-ResNets follows a simple procedure, depicted in Fig. 1. As shown in the transition from row (a) to (b) within Fig. 1, indices of partitioned layers within the global model are randomly permuted and distributed to sub-ResNets in a round-robin fashion. Each sub-ResNet receives an equal number of convolutional blocks (e.g., see row (b) within Fig. 1). In certain cases, residual blocks may be simultaneously partitioned to multiple sub-ResNets to ensure sufficient depth (e.g., see (★) in Fig. 1). ResIST produces subnetworks with $O(\frac{1}{S})$ of the global model depth, where S represents the number of independently-trained sub-ResNets.¹ To contrast this with existing non-distributed attempts, stochastic depth networks [28] have an expected depth of 75% of the global model.

¹A fixed number of blocks are excluded from partitioning (i.e., blocks not in the third section). As a result, this approximation of $O(\frac{1}{S})$ becomes more accurate as the network becomes deeper (i.e., deeper ResNet variants only add blocks to the third section), as a larger ratio of total blocks are included in the partitioning process.

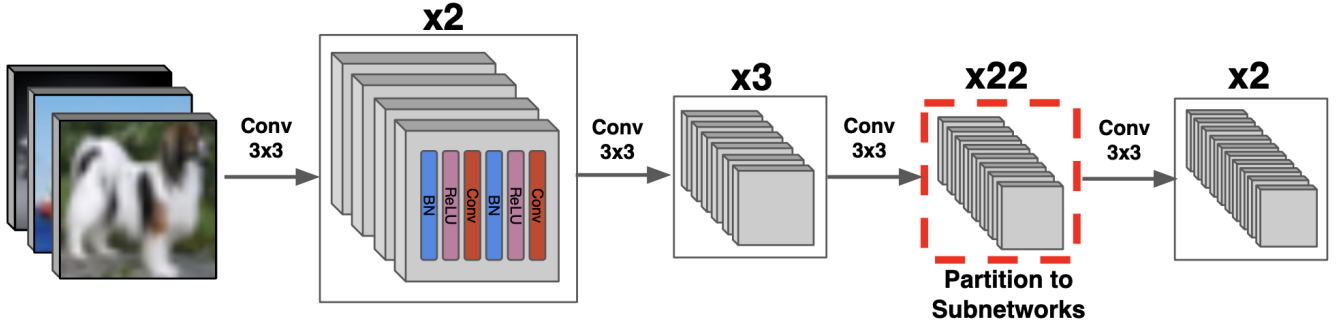


Figure 2: The ResNet101 model used in the majority of experiments. The figure identifies the convolutional blocks that are partitioned to subnetworks. The plot depicts the pre-activation ResNet setting, where we use BN, ReLU, and Conv layers twice in sequence. The network is comprised of four major “sections”, each containing a certain number of convolutional blocks of equal channel dimension.

The shallow sub-ResNets created by ResIST accelerate training and reduce communication in comparison to methods that communicate and train the full model. Table 1 shows the comparison of local SGD to ResIST with respect to the amount of data communicated during each synchronization round for different numbers of machines, highlighting the superior communication-efficiency of ResIST.

Table 1: Reports the amount of data communicated during each communication round (in GB) of both local SGD [60] and ResIST across different numbers of machines with ResNet101.

Method	2 Machine	4 Machine	8 Machine
Local SGD	0.662 GB	1.325 GB	2.649 GB
ResIST	0.454 GB	0.720 GB	1.289 GB

2.3 Distributed Training

The ResIST training procedure is outlined in Algorithm 1. Sub-ResNet construction (i.e., $\text{subResNets}(\cdot)$ in Algorithm 1) follows the procedure outlined in Sec. 2.2. After constructing the sub-ResNets, they are trained independently in a distributed manner (i.e., each on separate GPUs with different batches of data) for ℓ iterations [43]. Following independent training, the updates from each sub-ResNet are aggregated into the global model. Aggregation (i.e., $\text{aggregate}(\cdot)$ in Algorithm 1) sets each global network parameter to its average value across the sub-ResNets to which it was partitioned. If a parameter is only partitioned to a single sub-ResNet, aggregation simplifies to copying the parameter into the global model. After aggregation, layers from the global model are re-partitioned randomly to create a new group of sub-ResNets, and this entire process is repeated.

2.4 Implementation Details

We provide an implementation of ResIST in PyTorch [50], using the NCCL communication package. We use basic broadcast

Algorithm 1 ResIST Meta Algorithm

Parameters: T synchronization iterations, S sub-ResNets, ℓ local iterations, W ResNet weights.
 $h(W) \leftarrow$ randomly initialized ResNet.
for $t = 0, \dots, T - 1$ **do**
 $\{h_s(W_s)\}_{s=1}^S = \text{subResNets}(h(W), S)$.
Distribute each $h_s(W_s)$ to a different worker.
for $s = 1, \dots, S$ **do**
Train $h_s(W_s)$ for ℓ iterations using local SGD.
end for
 $h(W) = \text{aggregate}(\{h_s(W_s)\}_{s=1}^S)$.
end for

and reduce operations for communicating blocks in the third section and all reduce for blocks in other sections. We adopt the same communication procedure for the local SGD baseline (i.e., broadcast and reduce for the third section and all reduce for others) to ensure fair comparison. *The implementation of ResIST is decentralized, meaning that it does not assume a single, central parameter server.*

As shown in Fig. 3, during the synchronization and repartition step following local training, each sub-ResNet will directly send each of its locally-updated blocks to the designated new sub-ResNet (i.e., the parameters are not sent to an intermediate parameter server). At any time step, each worker will only need sufficient memory to store a single sub-ResNet, thus limiting the memory requirements. Such a decentralized implementation allows parallel communication between sub-ResNets, which leads to further speedups by preventing any single machine from causing slowdowns due to communication bottlenecks in the distributed procedure. The implementation is easily scalable to eight or more machines, either on nodes with multiple GPUs or across distributed nodes with dedicated GPUs.

This work is focused on the algorithmic level of distributed ResNet training. ResIST significantly reduces the number of bits communicated at each synchronization round and accelerates local training with the use of shallow sub-ResNets. The authors are well-aware

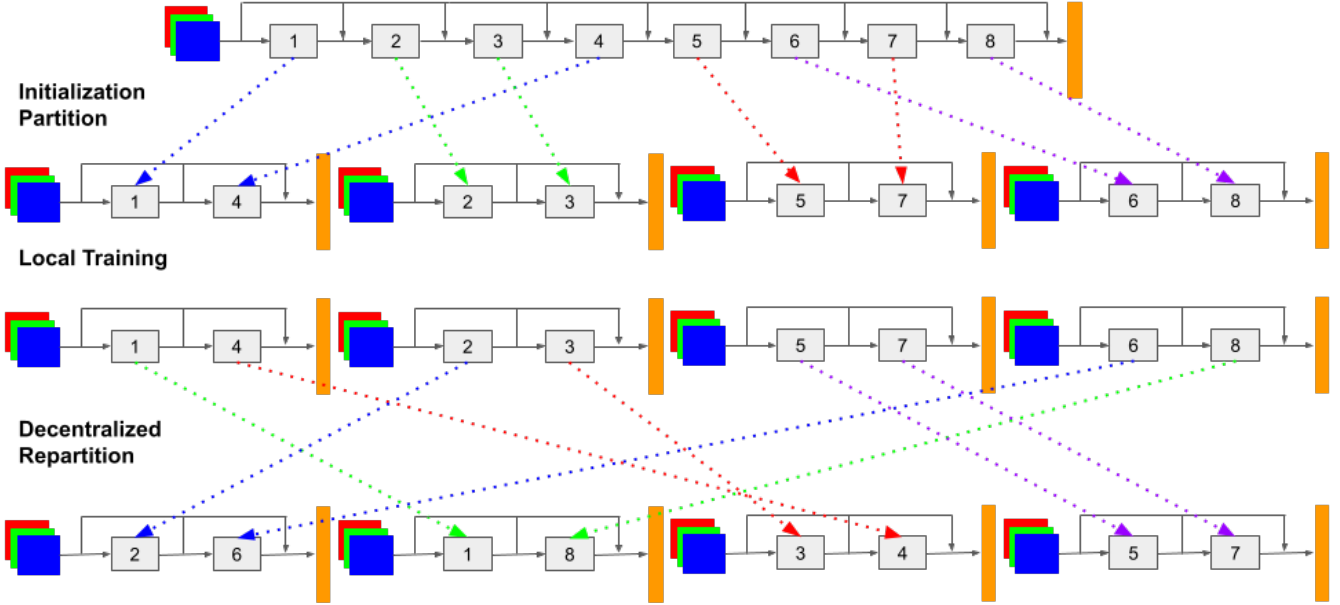


Figure 3: A depiction of the decentralized repartition procedure. This example partitions a ResNet with eight blocks into four different sub-ResNets. The “blue-green-red” squares dictate the data that lies per worker; the orange column dictates the last classification layer. As seen in the figure, each worker (from initialization partition to local training and decentralized repartition) is responsible for only a fraction of parameters of the whole network. The whole ResNet is never fully stored, communicated or updated on a single worker during training.

of many highly-optimized versions of data-parallel and synchronous training methodologies [20, 40, 56]. ResIST is fully compatible with these frameworks and can be further accelerated by leveraging highly-optimized distributed communication protocols at the systems level, which we leave as future work. Further, the authors are well-aware of advanced recent decentralized distributed computing techniques as in [6, 32, 36, 37, 41, 49, 64]; our goal is to showcase the benefits of our decomposition approach even on simpler distributed frameworks, and we leave the extension of ResIST to these more advanced protocols as future work.

2.5 Supplemental Techniques

Scaling Activations. Similar to [28], activations must be scaled appropriately to account for the full depth of the resulting network at test time. To handle this, the output of residual blocks in the third section of the network (see Fig. 2) are scaled by $1/S$, where S is the total number of sub-ResNets. Such scaling allows the global model to perform well, despite using all layers at test time.

Subnetwork Depth. Within ResIST, sub-ResNets may become too shallow as the number of sub-ResNets increases. To solve this issue, ResIST enforces a minimum depth requirement, which is satisfied by sharing certain blocks between multiple sub-ResNets. Through experimental analysis, a minimum of five blocks partitioned to each sub-ResNet was found to perform optimally. Such a finding motivates our choice of the ResNet101 architecture, as ResNet50

contains only five blocks for partitioning. ResIST is extensible to deeper architectures; see Sec. 6.4.

Tuning Local Iterations. We use a default value of $\ell = 50$, as $\ell < 50$ did not noticeably improve performance. In some cases, the performance of ResIST can be improved by tuning ℓ (see Fig. 6). The optimal setting of ℓ within ResIST is further explored in Sec. 6.3.

Local SGD Warm-up Phase. Directly applying ResIST may harm performance on some large-scale datasets (e.g., ImageNet). To solve this issue, we perform a few epochs with data parallel local SGD before training the model with ResIST.² By simply pre-training a model for a few epochs with local SGD, the remainder of training can be completed using ResIST without causing a significant performance decrease.

Maintaining Momentum Buffers. We use the SGD optimizer with momentum for all experiments.³ A global memory of the momentum buffer for each layer can be stored so that the buffer is maintained between synchronizations. This improves performance, but results in increased communication costs (i.e., the momentum buffer must be communicated between machines). As a result, we did not include this change within the final implementation of ResIST.

² Activations of blocks within the third section are still scaled during local SGD pre-training to maintain consistency with ResIST.

³ Experiments with different optimizers, such as Adam [34], AdamW [45], or Demon [11], do not show any improvements.

3 RELATED WORK

Following ResNet [24, 27, 44, 54], most novel architectures continued to leverage residual connections [55, 61], which became standard in most architectures [7, 15, 68]. The ResNet architecture has been further modified [26, 71, 80]. This work focuses on the pre-activation ResNet variant [26], as it achieves high performance and is well-suited to layer-wise decomposition.

The focus of this study is on synchronous methods of distributed optimization, such as data parallel training, parallel stochastic gradient descent (SGD) [2, 85], or local SGD [60]. Our methodology is also a variant of model-parallel training [8, 10, 19, 22, 23, 35, 51, 66, 84]. Many studies have explored possible techniques of synchronous, distributed optimization [42, 76, 83], yielding a wide number of viable variants [43], as well as techniques for MLP decomposition [79].

To reduce communication costs in the distributed setting, both quantization [4, 63, 77, 78] and sparsification [18, 31, 70] methods have been explored. Similarly, other studies have achieved speedups through the use of low-precision arithmetic during training [13, 30]. However, this line of work is orthogonal to our proposal and can be easily combined with the provided methodology; see Sec. 6.5.

Large batch training has been used to amortize communication and increase throughput for distributed training [21, 73]. The properties of large batch training have since been studied extensively [3, 33, 72, 75]. Large batches significantly alter training dynamics, warranting the use of complex heuristics to maintain comparable model performance [33, 72]. Here, we do not focus on the extension of ResIST to the large-batch training domain. Rather, we consider this as future work.

ResNet robustness to layer removal was explored in [28], while [69] showed that ensembles of shallow ResNets can yield high performance. [28] uses shallow networks during training and scales activations so that all layers may be used for inference. However, our approach is distinct in numerous ways. Primarily, our method partitions blocks in a stochastic, round-robin fashion, which explicitly prevents the exclusion of layers from training rounds and yields reduced subnetwork depth compared to [28]. Inspired by [39], we also selectively partition residual blocks that are least sensitive to pruning, allowing other layers (i.e., 30% of total layers) to be shared between subnetworks. Unlike [28], we avoid partitioning strided layers, which are sensitive to pruning [39]. Furthermore, our methodology, instead of proposing a form of regularization, focuses on utilizing independent training of shallow sub-ResNets for efficient, distributed training.

Our approach also relates to neural ODE literature. This area illustrates the ResNet as a discrete approximation to a continuous transformation from input image to output prediction [48]. The neural ODE perspective has been studied both empirically [12, 16, 46, 48] and theoretically [47, 59, 67]. This provides justification to our approach, as removing ResNet layers can be viewed as approximating the same transformation with a coarser discretization.

4 EXPERIMENTAL DETAILS

Hyperparameters are tuned using a holdout validation set and results are obtained using optimal hyperparameters from the validation set. All experiments are repeated for three trials, and the average performance is presented. We adopt local SGD as our baseline for synchronous, distributed training methods, as it is argued to be superior in comparison to vanilla data-parallel training [43]; see Sec. 2.4 for more details. We evaluate the proposed training methodology based on model performance and speed. *In all cases, ResIST achieves comparable performance to local SGD, while lowering the total wall-clock time of training.* We use AWS p3.8xlarge instances for experiments with two or four machines⁴ and p3.16xlarge instances for experiments with eight machines. We use each GPU as a single worker that hosts a different sub-ResNet.

Small-Scale Image Classification. Models are trained with ResIST on CIFAR10 and CIFAR100 for image classification. We adopt standard data augmentation techniques during training and testing [25]. We adopt a batch size of 128 for each worker. Training is conducted for 80 epochs for experiments with two machines and 160 epochs for experiments with four or eight machines. The recorded performance reflects the best test accuracy achieved throughout training, averaged across three separate trials. The total wall-clock training time is also reported for each experiment.

ImageNet Classification. Models are trained with ResIST on the 1,000-class ILSVRC2012 image classification dataset [14]. We adopt standard data augmentation techniques during training and testing, and use a batch size of 256 for each worker [25]. Training is conducted for 90 epochs. We initialize the learning rate to 0.1 and decrease it $10\times$ at epochs 30 and 60. For all experiments, we set $\ell = 15$, adopt a minimum depth of 10 blocks for each sub-ResNet, and warm-up pre-training using local SGD. For both ResIST and baseline experiments, we utilize momentum restarts and aggregate batch statistics every 1300 synchronization rounds.

Object Detection. ResIST is tested in the object detection domain on the Pascal VOC dataset [17]. Our model, inspired by the Yolo-v2 object detection model [53], consists of a ResNet101 backbone followed by a detection layer (i.e., a 1×1 convolution that outputs anchor box predictions). The ResNet backbone of this model is similar to the classification model described in Sec. 2.1, but without the pre-activation structure. The model is trained for 100 epochs with an image dimension of 448×448 and batch size of 10. No data augmentation techniques are used. The learning rate is increased from 10^{-5} to 10^{-4} over the first 30 epochs, and decreased by $10\times$ at epochs 60 and 90. Both Pascal VOC 2007 and 2012 training sets are used during training, and performance is evaluated on the Pascal VOC 2007 test set. We report the wall-clock training time and the best loss achieved on the test set throughout training. Experiments are conducted on two and four machines using both local SGD and ResIST.

⁴For Sec. 6.4 and Pascal VOC experiment with two machines, we use a cluster with eight V100 GPUs.

Table 2: Test accuracy of baseline LocalSGD versus ResIST on small-scale image classification datasets.

	# Machines	CIFAR10	CIFAR100
Local SGD	2	92.36% \pm 0.01	70.67% \pm 0.03
	4	92.90% \pm 0.06	71.51% \pm 0.04
	8	92.00% \pm 0.07	69.64% \pm 0.05
ResIST	2	91.95% \pm 0.32	70.06% \pm 0.51
	4	92.35% \pm 0.22	71.30% \pm 0.20
	8	91.45% \pm 0.30	70.26% \pm 0.21

5 RESULTS

5.1 Small-Scale Image Classification

Accuracy. The test accuracy of models trained with both ResIST and local SGD on small-scale image classification datasets is listed in Table 2. ResIST *achieves comparable test accuracy in all cases where the same number of machines are used.* Additionally, ResIST outperforms localSGD on CIFAR100 experiments with eight machines. The performance of ResIST and local SGD are strikingly similar in terms of test accuracy. In fact, the performance gap between the two method does not exceed 1% in any experimental setting. Furthermore, ResIST performance remains stable as the number of sub-ResNets increases, allowing greater acceleration to be achieved without degraded performance (e.g., see CIFAR100 results in Table 2). Generally, using four sub-ResNets yields the best performance with ResIST.

Efficiency. In addition to achieving comparable test accuracy to local SGD, ResIST significantly accelerates training. This acceleration is due to *i)* fewer parameters being communicated between machines and *ii)* locally-trained sub-ResNets being shallower than the global model. Wall-clock training times for four and eight machine experiments are presented in Tables 3. ResIST provides 3.58 to 3.81 \times speedup in comparison to local SGD. For eight machine experiments, a significant speedup over four machine experiments is not observed due to the minimum depth requirement and a reduction in the number of local iterations to improve training stability. We conjecture that for cases with higher communication cost at each synchronization and a similar number of synchronizations, eight worker ResIST could lead to more significant speedups in comparison to the four worker case.

A visualization of the speedup provided by ResIST on the CIFAR10 and CIFAR100 datasets is illustrated in Fig. 4. Models trained with ResIST match the final accuracy of those trained with local SGD. Furthermore, increasing the number of sub-ResNets yields an improved speedup for ResIST in comparison to localSGD. From these experiments, it is clear that the communication-efficiency of ResIST allows the benefit of more devices to be better realized in the distributed setting.

5.2 Large-Scale Image Classification

Accuracy. The test accuracy of models trained with both ResIST and local SGD for different numbers of machines on the ImageNet

Table 3: Total training time in seconds of baseline models and models trained with ResIST on small-scale image classification datasets.

	# Machines	Dataset	Total Time	Speedup
Local SGD	4	C10	5486 \pm 7.05	-
		C100	5528 \pm 65.90	-
	8	C10	10072 \pm 5.12	-
		C100	10058 \pm 8.71	-
ResIST	4	C10	1532 \pm 0.83	3.60\times
		C100	1545 \pm 1.27	3.58\times
	8	C10	2671 \pm 3.25	3.77\times
		C100	2639 \pm 3.89	3.81\times

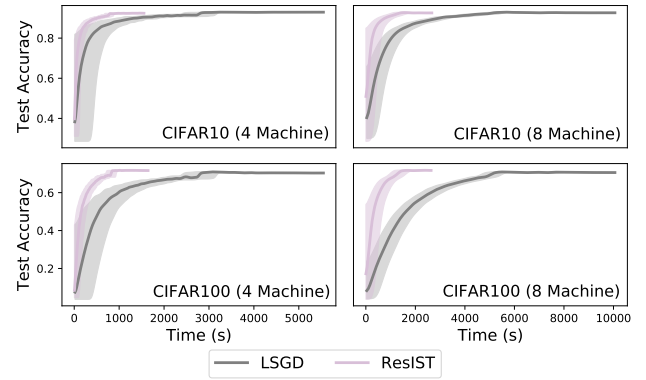


Figure 4: Both methodologies complete 160 epochs of training. Accuracy values are smoothed using a 1-D gaussian filter, and shaded regions represent deviations in accuracy.

dataset is listed in Table 4. As can be seen, ResIST *achieves comparable test accuracy (<2% difference) to local SGD in all cases where the same number of machines are used.* Additionally, as shown in [52], many current image classification models overfit to the ImageNet test set and cannot generalize well to new data. Thus, models trained with both local SGD and ResIST are also evaluated on three different ImageNet V2 testing sets [52]. As shown in Table 4, ResIST consistently achieves comparable test accuracy in comparison to local SGD on these supplemental test sets.

Efficiency. As shown in Tables 4 and 5, ResIST significantly accelerates the ImageNet training process. However, due to the use of fewer local iterations and the local SGD warm-up phase, the speedup provided by ResIST is smaller relative to experiments on small-scale datasets. In Table 4, it is shown that ResIST can reduce the total communication volume during training, which is an important feature in the implementation of distributed systems with high computational costs.

5.3 Object Detection

Loss. The test loss of models trained with both ResIST and local SGD for different numbers of machines on the Pascal VOC object

Table 4: Performance of baseline models and models trained with ResIST on 1K Imagenet. MF stands for test set “Matched-Frequency” and was sampled to match the MTurk selection frequency distribution of the original ImageNet validation set for each class; T-0.7 stands for test set “Threshold0.7” and was built by sampling ten images for each class among the candidates with selection frequency at least 0.7; TI stands for test set “TopImages” and contains the ten images with highest selection frequency in our candidate pool for each class. For more information, see [52].

	# Machines	Imagenet	Imagenet V2 Test Set			Training Time	Speedup	Communication	Cost Ratio
			MF	T-0.7	TI				
Local SGD	2	73.32%	60.72%	69.47%	75.48%	48.61 hours	-	7546.80 GB	-
	4	72.66%	59.88%	68.34%	74.27%	29.29 hours	-	7546.80 GB	-
ResIST	2	71.60%	58.92%	67.51%	73.56%	36.79 hours	1.32×	5831.2 GB	1.29×
	4	70.74%	57.56%	66.46%	72.65%	22.37 hours	1.31×	6007.6 GB	1.26×

Table 5: Total training time on Imagenet (in hours) of models trained with both local SGD and ResIST using two and four machines to reach a fixed test accuracy.

# Machines	Target Accuracy	Local SGD	ResIST	Speedup
2	71.00	33.26	26.63	1.25×
4	70.70	18.50	18.12	1.02×

detection dataset is listed in Table 6. Notably, ResIST achieves a lower test loss in comparison to local SGD for the experiment with two machines. Although the test loss achieved by ResIST is slightly worse than local SGD in the four machine case, the performance is comparable. Namely, the difference in test loss achieved by local SGD and ResIST never exceeds a value of one.

Efficiency. In addition to achieving comparable or improved test loss in comparison to local SGD, ResIST also provides a significant training acceleration on the PascalVOC dataset. In particular, models trained with ResIST achieve up to a 1.64× acceleration in comparison to object detection models trained with localSGD.

Table 6: Test loss and total training time on Pascal VOC for models trained with both local SGD and ResIST using two and four machines. Training time in seconds.

	# Machines	Test Loss	Training Time	Speedup
Local SGD	2	6.15 ± 0.03	39621 ± 9.12	-
	4	6.22 ± 0.06	16840 ± 0.11	-
ResIST	2	5.99 ± 0.01	24058 ± 3.22	1.64×
	4	6.69 ± 0.17	11264 ± 49.38	1.49×

6 ABLATIONS

These experiments aim to provide an understanding of the algorithm’s behavior, as well as provide empirical support for its design.

6.1 Designing ResIST

Extensive ablation experiments are conducted on the CIFAR10 dataset, outlined in Fig. 5, to empirically motivate the design choices made within ResIST (i.e., see Sec. 2.5). For the two sub-ResNet case,

the naive implementation of ResIST, which evenly splits all convolutional blocks between subnetworks, is shown to perform poorly (i.e., <70% on CIFAR10). The accuracy of ResIST is improved over 25% by only allowing select layers to be partitioned and ensuring activations are scaled correctly when performing inference with the full network. The pre-activation ResNet is shown to yield an improvement in accuracy, leading ResIST to perform near optimally with two sub-ResNets.

Modification	Naive Model						ResIST
Share strided layers		✓	✓	✓	✓	✓	✓
Only Partition Section 3			✓	✓	✓	✓	✓
Scale Activations				✓	✓	✓	✓
Pre-Act ResNet					✓	✓	✓
Minimum Depth						✓	✓
Tune Local Iterations							✓
2 Sub-ResNet Acc.	66.3%	68.3%	84.3%	91.5%	92.0%	-	92.0%
8 Sub-ResNet Acc.	-	-	-	-	86.5%	89.9%	91.3%

Figure 5: Depicts the test accuracies on the CIFAR10 dataset for a single run for the major ablation experiments performed with ResIST.

When ResIST is expanded to eight sub-ResNets, we initially observe a significant decrease in model accuracy. However, as can be seen in Fig. 5, this gap can be closed by enforcing a minimum depth on sub-ResNets and tuning the number of local iterations. By making these extra modifications, ResIST begins to perform similarly with two to eight sub-ResNets, yielding compelling performance.

6.2 Shallow Ensembles

The ResIST algorithm requires that independently-trained sub-ResNets must have their parameters synchronized intermittently.

Such synchronization, however, can be completely avoided by training each sub-ResNet separately and forming an ensemble (i.e., ResIST without any aggregation). Although maintaining an ensemble has several drawbacks (e.g., slower inference, more parameters, etc.), the training time of the ensemble would nonetheless be reduced in comparison to ResIST by avoiding communication altogether. Therefore, the performance of such an ensemble should be compared to the models trained with ResIST.

Table 7: Performance of independently-trained ensembles of shallow ResNets in comparison to ResIST on CIFAR10 and CIFAR100 (denoted as C10 and C100, respectively).

Dataset	Method	2 Model	4 Model	8 Model
C10	Ensemble	92.27 % \pm 0.00	92.56% \pm 0.03	90.67 % \pm 0.04
	ResIST	91.95% \pm 0.32	92.35% \pm 0.22	91.45% \pm 0.30
C100	Ensemble	72.08% \pm 0.05	72.12% \pm 0.04	67.98 % \pm 0.12
	ResIST	70.06% \pm 0.51	71.30% \pm 0.20	70.26% \pm 0.21

The performance of sub-ResNet ensembles in comparison to models trained with ResIST is displayed in Table 7. For 8 Sub-ResNets, the shallow ensembles achieve inferior performance in comparison to ResIST. When two and four Sub-ResNets are used, the performance of shallow ensembles and ResIST is comparable (i.e., $< 1\%$ performance difference in most cases). However, it should be noted that such shallow ensembles of two or four sub-ResNets, in comparison to models trained with ResIST, cause a $2\times$ to $4\times$ slowdown in inference time (i.e., inference time for a single Sub-ResNet is not significantly faster than that of the global ResNet). Furthermore, the ensembles consume more parameters in comparison to global ResNet trained with ResIST.

6.3 Robustness to Local Iterations

ResIST is robust to various numbers of local iterations [9, 43, 82]. An extensive sweep over possible values of ℓ is performed on CIFAR100. The results of this experiment are depicted in Fig. 6. As can be seen, ResIST achieves high accuracy even with thousands of local SGD iterations (i.e., previous work typically uses much fewer [43]). However, if more sub-ResNets are used, performance tends to deteriorate more quickly as local iterations increase. Due to the robustness of ResIST to large numbers of local iterations, training can be accelerated without deteriorating model performance by simply increasing the value of ℓ . Local SGD was found to demonstrate similar robustness to the number of local iterations, as shown in Fig. 6.

6.4 Deeper architectures

The ResIST methodology is easily applicable to deeper architectures. To demonstrate this, results are replicated for CIFAR10 and CIFAR100 datasets with ResNet152 and ResNet200. These deeper architectures are identical to the original ResNet101 architecture (i.e., see Fig. 2). However, more residual blocks are added to the third section of the ResNet (i.e., the highlighted portion of Fig. 2) to increase the model’s depth. It should be noted that convolutional blocks within the third section of the ResNet are partitioned in

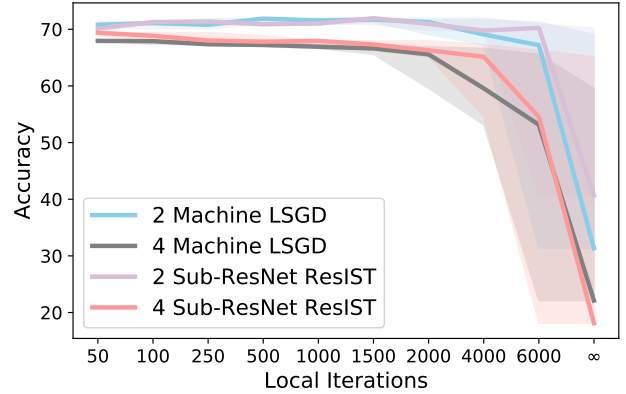


Figure 6: Test accuracy on CIFAR100 for ResNet-101 trained with both ResIST and local SGD (LSGD) with different numbers of local iterations. ∞ local iterations refers to aggregating parameters only once at the end of training (i.e., single-shot averaging). Shaded regions reflect deviations in accuracy.

ResIST by default (see Sec. 2.2). As a result, all extra residual blocks within these deeper architectures are partitioned to sub-ResNets by ResIST (i.e., no extra blocks are shared between sub-ResNets), allowing ResIST to achieve greater acceleration in comparison to local SGD.

The results of experiments with deeper ResNets are presented in Table 8. ResIST performs competitively with localSGD in all cases. Furthermore, ResIST achieves a significant speedup in comparison to local SGD that becomes more pronounced as the model becomes deeper. E.g., for 4-GPUs, ResIST completes training $> 3\times$ faster than local SGD for ResNet200 on both datasets. This speedup is caused by a greater ratio of total network blocks being partitioned to sub-ResNets in ResIST. While local SGD must communicate all parameters between machines, ResIST achieves a relative decrease in communication by partitioning all extra residual blocks evenly between sub-ResNets.

6.5 ResIST with Quantization and Gradient Sparsification

Many quantization [4, 78] and sparsification [18, 31] techniques have been proposed for reducing communication costs in distributed training. Such techniques focus on compressing communicated data, and they do not interfere with our methodology, which provides a novel approach to model synchronization and training. The proposed approach can be easily combined with existing compression techniques to further reduce communication costs and accelerate training *with no extra tuning or modifications*. To demonstrate that ResIST works well with quantization, we compress all communicated parameters using both four-bit and eight-bit compression. Table 9 shows that ResIST retains its performance until the compression level reaches five-bit and lower. We also perform experiments with sparsification of communicated weights by only keeping 25% of total weights within each synchronization round.

Table 8: Test accuracy on CIFAR10 (C10) and CIFAR100 (C100) for deeper architectures trained with ResIST and local SGD (LSGD). All tests were performed with 100 local iterations between synchronization rounds. All models were trained for 80 epochs.

Dataset	# Machines	Method	ResNet152			ResNet200		
			Time	Test Acc.	Speedup	Time	Test Acc.	Speedup
C10	2	LSGD	3512s	92.27% \pm 0.003		4575s	92.31% \pm 0.001	
		ResIST	2215s	92.01% \pm 0.002	1.58\times	2380s	92.10% \pm 0.001	1.92\times
	4	LSGD	3598s	91.39% \pm 0.001		4357s	91.35% \pm 0.000	
		ResIST	1054s	90.67% \pm 0.001	3.41\times	1161s	90.27% \pm 0.001	3.75\times
C100	2	LSGD	3528s	70.50% \pm 0.003		4639s	71.05% \pm 0.005	
		ResIST	2291s	70.32% \pm 0.005	1.53\times	2202s	70.71% \pm 0.002	2.10\times
	4	LSGD	3518s	68.39% \pm 0.004		4391s	69.05% \pm 0.003	
		ResIST	1164s	67.27% \pm 0.003	3.02\times	1195s	67.62% \pm 0.001	3.67\times

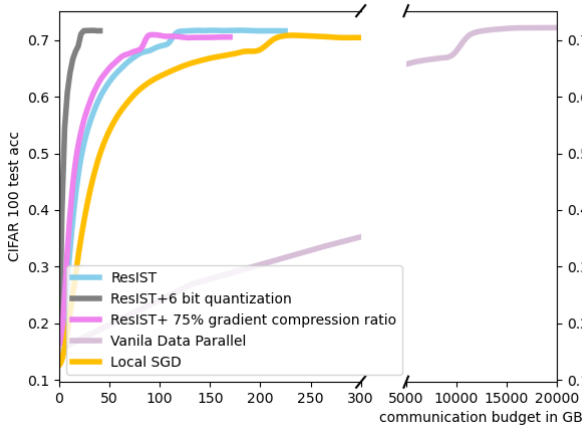


Figure 7: Test accuracy vs. communication budget for ResIST, ResIST+quantization, ResIST+gradient compression, local SGD and vanilla data parallel on CIFAR100. All models are trained over a 4-GPU cluster.

Such a strategy reaches a validation performance of 71.25% on CIFAR100. We summarize the results of all quantization experiments in Fig. 7, where we compare communication budgets across different compression techniques with ResIST. From this figure, it is clear that ResIST is most efficient with six-bit quantization and is compatible with most main-stream compression techniques.

Table 9: Test Accuracy for ResIST combined with quantization on CIFAR10 and CIFAR100 (denoted as C10 and C100, respectively).

Dataset	8 bit	7 bit	6 bit	5 bit	4 bit
C10	92.14%	92.26%	91.91%	91.35%	76.33%
C100	71.38%	72.15%	71.37%	68.29%	40.48%

7 CONCLUSION

In the work, we present ResIST, a novel algorithm for synchronous, distributed training of ResNets. ResIST operates by decomposing a global ResNet model into several shallower sub-ResNets, which are trained independently and intermittently aggregated into the global model. By only communicating parameters of sub-ResNets between machines and training shallower, less expensive networks, ResIST reduces the communication and local training cost of synchronous, distributed training. We demonstrate the impact of ResIST on several image classification datasets, as well as in the object detection domain, by highlighting the significant training acceleration it provides in comparison to methods like local SGD [43] without any deterioration in performance.

In the future, we aim to extend ResIST to other network architectures, as ResIST is fully-extensible to all network architectures with residual connections. Because residual connections are now standard in most important deep learning architectures (e.g., transformers [7, 15, 68]), many opportunities to extend applications of ResIST exist within this domain. On the other hand, ResIST has been shown to be fully-compatible with various gradient compression methods. As such, we will investigate the prospect of fully integrating such compression methods within ResIST, both during training and communication phases, to further decrease memory and computation costs.

ACKNOWLEDGEMENTS

AK and CJ acknowledge funding by the NSF (CCF-1907936).

REFERENCES

- [1] Martín Abadi, Ashish Agarwal, Paul Barham, Eugene Brevdo, Zhifeng Chen, Craig Citro, Greg S. Corrado, Andy Davis, Jeffrey Dean, Matthieu Devin, Sanjay Ghemawat, Ian Goodfellow, Andrew Harp, Geoffrey Irving, Michael Isard, Yangqing Jia, Rafal Jozefowicz, Lukasz Kaiser, Manjunath Kudlur, Josh Levenberg, Dan Mané, Rajat Monga, Sherry Moore, Derek Murray, Chris Olah, Mike Schuster, Jonathon Shlens, Benoit Steiner, Ilya Sutskever, Kunal Talwar, Paul Tucker, Vincent Vanhoucke, Vijay Vasudevan, Fernanda Viégas, Oriol Vinyals, Pete Warden, Martin Wattenberg, Martin Wicke, Yuan Yu, and Xiaoqiang Zheng. 2015. TensorFlow: Large-Scale Machine Learning on Heterogeneous Systems.
- [2] Alekh Agarwal and John C Duchi. 2011. Distributed delayed stochastic optimization. In *Advances in Neural Information Processing Systems*. 873–881.
- [3] Takuya Akiba, Shuji Suzuki, and Keisuke Fukuda. 2017. Extremely large minibatch sgd: Training resnet-50 on imagenet in 15 minutes. *arXiv preprint arXiv:1711.04325* (2017).

- [4] Dan Alistarh, Demjan Grubic, Jerry Li, Ryota Tomioka, and Milan Vojnovic. 2016. QSGD: Communication-Efficient SGD via Gradient Quantization and Encoding. *arXiv e-prints*, Article arXiv:1610.02132 (Oct. 2016), arXiv:1610.02132 pages. arXiv:cs.LG/1610.02132
- [5] Mahmoud Assran, Arda Aytetin, Hamid Feyzmahdavian, Mikael Johansson, and Michael Rabbat. 2020. Advances in Asynchronous Parallel and Distributed Optimization. *arXiv e-prints*, Article arXiv:2006.13838 (June 2020), arXiv:2006.13838 pages. arXiv:cs.LG/2006.13838
- [6] Mahmoud Assran and Michael Rabbat. 2020. Asynchronous gradient-push. *IEEE Trans. Automat. Control* (2020).
- [7] Thomas Bachlechner, Bodhisattwa Prasad Majumder, Huanru Henry Mao, Garrison W Cottrell, and Julian McAuley. 2020. Rezero is all you need: Fast convergence at large depth. *arXiv preprint arXiv:2003.04887* (2020).
- [8] Tal Ben-Nun and Torsten Hoefler. 2018. Demystifying Parallel and Distributed Deep Learning: An In-Depth Concurrency Analysis. *arXiv e-prints*, Article arXiv:1802.09941 (Feb. 2018), arXiv:1802.09941 pages. arXiv:cs.LG/1802.09941
- [9] H. Brendan McMahan, Eider Moore, Daniel Ramage, Seth Hampson, and Blaise Agüera y Arcas. 2016. Communication-Efficient Learning of Deep Networks from Decentralized Data. *arXiv e-prints*, Article arXiv:1602.05629 (Feb. 2016), arXiv:1602.05629 pages. arXiv:cs.LG/1602.05629
- [10] Chi-Chung Chen, Chia-Lin Yang, and Hsiang-Yun Cheng. 2018. Efficient and Robust Parallel DNN Training through Model Parallelism on Multi-GPU Platform. *arXiv e-prints*, Article arXiv:1809.02839 (Sept. 2018), arXiv:1809.02839 pages. arXiv:cs.DC/1809.02839
- [11] John Chen, Cameron Wolfe, Zhao Li, and Anastasios Kyrillidis. 2019. Demon: Momentum Decay for Improved Neural Network Training. *arXiv e-prints*, Article arXiv:1910.04952 (Oct. 2019), arXiv:1910.04952 pages. arXiv:cs.LG/1910.04952
- [12] Ricky T. Q. Chen, Yulia Rubanova, Jesse Bettencourt, and David Duvenaud. 2018. Neural Ordinary Differential Equations. *arXiv e-prints*, Article arXiv:1806.07366 (June 2018), arXiv:1806.07366 pages. arXiv:cs.LG/1806.07366
- [13] Christopher De Sa, Megan Leszczynski, Jian Zhang, Alana Marzoev, Christopher R. Aberger, Kunle Olukotun, and Christopher Ré. 2018. High-Accuracy Low-Precision Training. *arXiv e-prints*, Article arXiv:1803.03383 (March 2018), arXiv:1803.03383 pages. arXiv:cs.LG/1803.03383
- [14] Jia Deng, Wei Dong, Richard Socher, Li-Jia Li, Kai Li, and Li Fei-Fei. 2009. Imagenet: A large-scale hierarchical image database. In *2009 IEEE conference on computer vision and pattern recognition*. Ieee, 248–255.
- [15] Jacob Devlin, Ming-Wei Chang, Kenton Lee, and Kristina Toutanova. 2018. Bert: Pre-training of deep bidirectional transformers for language understanding. *arXiv preprint arXiv:1810.04805* (2018).
- [16] Emilien Dupont, Arnaud Doucet, and Yee Whye Teh. 2019. Augmented neural odes. In *Advances in Neural Information Processing Systems*. 3140–3150.
- [17] Mark Everingham, Luc Van Gool, Christopher KI Williams, John Winn, and Andrew Zisserman. 2010. The pascal visual object classes (voc) challenge. *International journal of computer vision* 88, 2 (2010), 303–338.
- [18] Alham Fikri Aji and Kenneth Heafield. 2017. Sparse Communication for Distributed Gradient Descent. *arXiv e-prints*, Article arXiv:1704.05021 (April 2017), arXiv:1704.05021 pages. arXiv:cs.CL/1704.05021
- [19] Amir Gholami, Arifur Azad, Peter Jin, Kurt Keutzer, and Aydin Buluc. 2017. Integrated Model, Batch and Domain Parallelism in Training Neural Networks. *arXiv e-prints*, Article arXiv:1712.04432 (Dec. 2017), arXiv:1712.04432 pages. arXiv:cs.LG/1712.04432
- [20] Google. 2020. *Distributed Training with TensorFlow*. https://www.tensorflow.org/guide/distributed_training
- [21] Priya Goyal, Piotr Dollár, Ross Girshick, Pieter Noordhuis, Lukasz Wesolowski, Aapo Kyrola, Andrew Tulloch, Yangqing Jia, and Kaiming He. 2017. Accurate, large minibatch sgd: Training imagenet in 1 hour. *arXiv preprint arXiv:1706.02677* (2017).
- [22] Lei Guan, Wotao Yin, Dongsheng Li, and Xicheng Lu. 2019. XPipe: Efficient Pipeline Model Parallelism for Multi-GPU DNN Training. *arXiv e-prints*, Article arXiv:1911.04610 (Oct. 2019), arXiv:1911.04610 pages. arXiv:cs.LG/1911.04610
- [23] S. Günther, L. Ruthotto, J. B. Schroder, E. C. Cyr, and N. R. Gauger. 2018. Layer-Parallel Training of Deep Residual Neural Networks. *arXiv e-prints*, Article arXiv:1812.04352 (Dec. 2018), arXiv:1812.04352 pages. arXiv:math.OA/1812.04352
- [24] Kaiming He, Georgia Gkioxari, Piotr Dollár, and Ross Girshick. 2017. Mask r-cnn. In *Proceedings of the IEEE international conference on computer vision*. 2961–2969.
- [25] Kaiming He, Xiangyu Zhang, Shaoqing Ren, and Jian Sun. 2016. Deep residual learning for image recognition. In *Proceedings of the IEEE conference on computer vision and pattern recognition*. 770–778.
- [26] Kaiming He, Xiangyu Zhang, Shaoqing Ren, and Jian Sun. 2016. Identity mappings in deep residual networks. In *European conference on computer vision*. Springer, 630–645.
- [27] Gao Huang, Zhuang Liu, Laurens Van Der Maaten, and Kilian Q Weinberger. 2017. Densely connected convolutional networks. In *Proceedings of the IEEE conference on computer vision and pattern recognition*. 4700–4708.
- [28] Gao Huang, Yu Sun, Zhuang Liu, Daniel Sedra, and Kilian Q. Weinberger. 2016. Deep Networks with Stochastic Depth. *CoRR abs/1603.09382* (2016), arXiv:1603.09382 <http://arxiv.org/abs/1603.09382>
- [29] Sergey Ioffe and Christian Szegedy. 2015. Batch normalization: Accelerating deep network training by reducing internal covariate shift. *arXiv preprint arXiv:1502.03167* (2015).
- [30] Xianyan Jia, Shutao Song, Wei He, Yangzihao Wang, Haidong Rong, Feihu Zhou, Liqiang Xie, Zhenyu Guo, Yuanzhou Yang, Liwei Yu, et al. 2018. Highly scalable deep learning training system with mixed-precision: Training imagenet in four minutes. *arXiv preprint arXiv:1807.11205* (2018).
- [31] Peng Jiang and Gagan Agrawal. 2018. A Linear Speedup Analysis of Distributed Deep Learning with Sparse and Quantized Communication. In *Advances in Neural Information Processing Systems 31*, S. Bengio, H. Wallach, H. Larochelle, K. Grauman, N. Cesa-Bianchi, and R. Garnett (Eds.). Curran Associates, Inc., 2525–2536.
- [32] Björn Johansson, Maben Rabi, and Mikael Johansson. 2010. A randomized incremental subgradient method for distributed optimization in networked systems. *SIAM Journal on Optimization* 20, 3 (2010), 1157–1170.
- [33] Tyler B Johnson, Pulkit Agrawal, Haijie Gu, and Carlos Guestrin. 2020. AdaScale SGD: A User-Friendly Algorithm for Distributed Training. *arXiv preprint arXiv:2007.05105* (2020).
- [34] Diederik P. Kingma and Jimmy Ba. 2014. Adam: A Method for Stochastic Optimization. *arXiv e-prints*, Article arXiv:1412.6980 (Dec. 2014), arXiv:1412.6980 pages. arXiv:cs.LG/1412.6980
- [35] Andrew C. Kirby, Siddharth Samsi, Michael Jones, Albert Reuther, Jeremy Kepner, and Vijay Gadepally. 2020. Layer-Parallel Training with GPU Concurrency of Deep Residual Neural Networks via Nonlinear Multigrid. *arXiv e-prints*, Article arXiv:2007.07336 (July 2020), arXiv:2007.07336 pages. arXiv:cs.LG/2007.07336
- [36] Anastasia Koloskova, Nicolas Loizou, Sadra Boreiri, Martin Jaggi, and Sebastian Stich. 2020. A unified theory of decentralized SGD with changing topology and local updates. In *International Conference on Machine Learning*. PMLR, 5381–5393.
- [37] Anastasia Koloskova, Sebastian Stich, and Martin Jaggi. 2019. Decentralized stochastic optimization and gossip algorithms with compressed communication. In *International Conference on Machine Learning*. PMLR, 3478–3487.
- [38] Alex Krizhevsky, Ilya Sutskever, and Geoffrey E Hinton. 2012. Imagenet classification with deep convolutional neural networks. In *Advances in neural information processing systems*. 1097–1105.
- [39] Hao Li, Asim Kadav, Igor Durdanovic, Hanan Samet, and Hans Peter Graf. 2016. Pruning Filters for Efficient ConvNets. *arXiv e-prints*, Article arXiv:1608.08710 (Aug. 2016), arXiv:1608.08710 pages. arXiv:cs.CV/1608.08710
- [40] Shen Li. 2017. *Getting Started with Distributed Data Parallel*. https://pytorch.org/tutorials/intermediate/ddp_tutorial.html
- [41] Xiangru Lian, Ce Zhang, Huan Zhang, Cho-Jui Hsieh, Wei Zhang, and Ji Liu. 2017. Can decentralized algorithms outperform centralized algorithms? a case study for decentralized parallel stochastic gradient descent. *arXiv preprint arXiv:1705.09056* (2017).
- [42] Xiangru Lian, Ce Zhang, Huan Zhang, Cho-Jui Hsieh, Wei Zhang, and Ji Liu. 2017. Can decentralized algorithms outperform centralized algorithms? a case study for decentralized parallel stochastic gradient descent. In *Advances in Neural Information Processing Systems*. 5330–5340.
- [43] Tao Lin, Sebastian U. Stich, Kumar Kshitij Patel, and Martin Jaggi. 2018. Don't Use Large Mini-Batches, Use Local SGD. *arXiv e-prints*, Article arXiv:1808.07217 (Aug. 2018), arXiv:1808.07217 pages. arXiv:cs.LG/1808.07217
- [44] Tsung-Yi Lin, Priya Goyal, Ross Girshick, Kaiming He, and Piotr Dollár. 2017. Focal loss for dense object detection. In *Proceedings of the IEEE international conference on computer vision*. 2980–2988.
- [45] Ilya Loshchilov and Frank Hutter. 2017. Decoupled Weight Decay Regularization. *arXiv e-prints*, Article arXiv:1711.05101 (Nov. 2017), arXiv:1711.05101 pages. arXiv:cs.LG/1711.05101
- [46] Yiping Lu, Zhuohan Li, Di He, Zhiqing Sun, Bin Dong, Tao Qin, Liwei Wang, and Tie-Yan Liu. 2019. Understanding and Improving Transformer From a Multi-Particle Dynamic System Point of View. *arXiv e-prints*, Article arXiv:1906.02762 (June 2019), arXiv:1906.02762 pages. arXiv:cs.LG/1906.02762
- [47] Yiping Lu, Chao Ma, Yulong Lu, Jianfeng Lu, and Lexing Ying. 2020. A Mean-field Analysis of Deep ResNet and Beyond: Towards Provable Optimization Via Overparameterization From Depth. *arXiv e-prints*, Article arXiv:2003.05508 (March 2020), arXiv:2003.05508 pages. arXiv:stat.ML/2003.05508
- [48] Yiping Lu, Aoxiao Zhong, Quanzheng Li, and Bin Dong. 2018. Beyond finite layer neural networks: Bridging deep architectures and numerical differential equations. In *International Conference on Machine Learning*. PMLR, 3276–3285.
- [49] Angelia Nedic and Asuman Ozdaglar. 2009. Distributed subgradient methods for multi-agent optimization. *IEEE Trans. Automat. Control* 54, 1 (2009), 48–61.
- [50] Adam Paszke, Sam Gross, Francisco Massa, Adam Lerer, James Bradbury, Gregory Chanan, Trevor Killeen, Zeming Lin, Natalia Gimelshein, Luca Antiga, Alban Desmaison, Andreas Kopf, Edward Yang, Zachary DeVito, Martin Raison, Alykhan Tejani, Sasank Chilamkurthy, Benoit Steiner, Lu Fang, Junjie Bai, and Soumith Chintala. 2019. PyTorch: An Imperative Style, High-Performance Deep Learning Library. In *Advances in Neural Information Processing Systems 32*, H. Wallach, H. Larochelle, A. Beygelzimer, F. d'Alché-Buc, E. Fox, and R. Garnett (Eds.). Curran Associates, Inc., 8024–8035.

- [51] J. Gregory Pauloski, Zhao Zhang, Lei Huang, Weijia Xu, and Ian T. Foster. 2020. Convolutional Neural Network Training with Distributed K-FAC. *arXiv e-prints*, Article arXiv:2007.00784 (July 2020), arXiv:2007.00784 pages. arXiv:cs.LG/2007.00784
- [52] Benjamin Recht, Rebecca Roelofs, Ludwig Schmidt, and Vaishaal Shankar. 2019. Do imagenet classifiers generalize to imagenet?. In *International Conference on Machine Learning*. PMLR, 5389–5400.
- [53] Joseph Redmon and Ali Farhadi. 2016. YOLO9000: Better, Faster, Stronger. *arXiv e-prints*, Article arXiv:1612.08242 (Dec. 2016), arXiv:1612.08242 pages. arXiv:cs.CV/1612.08242
- [54] Shaoqing Ren, Kaiming He, Ross Girshick, and Jian Sun. 2015. Faster r-cnn: Towards real-time object detection with region proposal networks. In *Advances in neural information processing systems*. 91–99.
- [55] Mark Sandler, Andrew Howard, Menglong Zhu, Andrey Zhmoginov, and Liang-Chieh Chen. 2018. Mobilenetv2: Inverted residuals and linear bottlenecks. In *Proceedings of the IEEE conference on computer vision and pattern recognition*. 4510–4520.
- [56] Alexander Sergeev and Mike Del Balso. 2018. Horovod: fast and easy distributed deep learning in TensorFlow. *arXiv preprint arXiv:1802.05799* (2018).
- [57] Shao-huai Shi, Qiang Wang, and Xiao-wen Chu. 2017. Performance Modeling and Evaluation of Distributed Deep Learning Frameworks on GPUs. *arXiv e-prints*, Article arXiv:1711.05979 (Nov. 2017), arXiv:1711.05979 pages. arXiv:cs.DC/1711.05979
- [58] Karen Simonyan and Andrew Zisserman. 2014. Very deep convolutional networks for large-scale image recognition. *arXiv preprint arXiv:1409.1556* (2014).
- [59] Sho Sonoda and Noboru Murata. 2017. Double continuum limit of deep neural networks. In *ICML Workshop Principled Approaches to Deep Learning*, Vol. 1740.
- [60] Sebastian U. Stich. 2019. Local SGD Converges Fast and Communicates Little. In *International Conference on Learning Representations*. <https://openreview.net/forum?id=S1g2JnRcFX>
- [61] Christian Szegedy, Sergey Ioffe, Vincent Vanhoucke, and Alex Alemi. 2016. Inception-v4, inception-resnet and the impact of residual connections on learning. *arXiv preprint arXiv:1602.07261* (2016).
- [62] Christian Szegedy, Wei Liu, Yangqing Jia, Pierre Sermanet, Scott Reed, Dragomir Anguelov, Dumitru Erhan, Vincent Vanhoucke, and Andrew Rabinovich. 2015. Going deeper with convolutions. In *Proceedings of the IEEE conference on computer vision and pattern recognition*. 1–9.
- [63] Hanlin Tang, Shao-duo Gan, Ce Zhang, Tong Zhang, and Ji Liu. 2018. Communication Compression for Decentralized Training. *arXiv e-prints*, Article arXiv:1803.06443 (March 2018), arXiv:1803.06443 pages. arXiv:cs.LG/1803.06443
- [64] Hanlin Tang, Xiangru Lian, Ming Yan, Ce Zhang, and Ji Liu. 2018. D^2 : Decentralized training over decentralized data. In *International Conference on Machine Learning*. PMLR, 4848–4856.
- [65] Zhenheng Tang, Shao-huai Shi, Xiao-wen Chu, Wei Wang, and Bo Li. 2020. Communication-Efficient Distributed Deep Learning: A Comprehensive Survey. *arXiv e-prints*, Article arXiv:2003.06307 (March 2020), arXiv:2003.06307 pages. arXiv:cs.DC/2003.06307
- [66] Sanket Tavarageri, Srinivas Sridharan, and Bharat Kaul. 2019. Automatic Model Parallelism for Deep Neural Networks with Compiler and Hardware Support. *arXiv e-prints*, Article arXiv:1906.08168 (June 2019), arXiv:1906.08168 pages. arXiv:cs.DC/1906.08168
- [67] Matthew Thorpe and Yves van Gennip. 2018. Deep limits of residual neural networks. *arXiv preprint arXiv:1810.11741* (2018).
- [68] Ashish Vaswani, Noam Shazeer, Niki Parmar, Jakob Uszkoreit, Llion Jones, Aidan N Gomez, Łukasz Kaiser, and Illia Polosukhin. 2017. Attention is all you need. In *Advances in neural information processing systems*. 5998–6008.
- [69] Andreas Veit, Michael Wilber, and Serge Belongie. 2016. Residual Networks Behave Like Ensembles of Relatively Shallow Networks. *arXiv e-prints*, Article arXiv:1605.06431 (May 2016), arXiv:1605.06431 pages. arXiv:cs.CV/1605.06431
- [70] Jianqiao Wangni, Jialei Wang, Ji Liu, and Tong Zhang. 2018. Gradient Sparsification for Communication-Efficient Distributed Optimization. In *Advances in Neural Information Processing Systems 31*, S. Bengio, H. Wallach, H. Larochelle, K. Grauman, N. Cesa-Bianchi, and R. Garnett (Eds.). Curran Associates, Inc., 1299–1309.
- [71] Saining Xie, Ross Girshick, Piotr Dollár, Zhuowen Tu, and Kaiming He. 2016. Aggregated Residual Transformations for Deep Neural Networks. *arXiv e-prints*, Article arXiv:1611.05431 (Nov. 2016), arXiv:1611.05431 pages. arXiv:cs.CV/1611.05431
- [72] Yang You, Igor Gitman, and Boris Ginsburg. 2017. Scaling sgd batch size to 32k for imagenet training. *arXiv preprint arXiv:1708.03888* 6 (2017).
- [73] Yang You, Jing Li, Sashank Reddi, Jonathan Hseu, Sanjiv Kumar, Srinadh Bhojanapalli, Xiaodan Song, James Demmel, Kurt Keutzer, and Cho-Jui Hsieh. 2019. Large batch optimization for deep learning: Training bert in 76 minutes. *arXiv preprint arXiv:1904.00962* (2019).
- [74] Yang You, Zhao Zhang, Cho-Jui Hsieh, James Demmel, and Kurt Keutzer. 2018. Imagenet training in minutes. In *Proceedings of the 47th International Conference on Parallel Processing*. 1–10.
- [75] Yang You, Zhao Zhang, Cho-Jui Hsieh, James Demmel, and Kurt Keutzer. 2018. Imagenet training in minutes. In *Proceedings of the 47th International Conference on Parallel Processing*. 1–10.
- [76] Kwangmin Yu, Thomas Flynn, Shinjae Yoo, and Nicholas D’Imperio. 2019. Layered SGD: A Decentralized and Synchronous SGD Algorithm for Scalable Deep Neural Network Training. *arXiv preprint arXiv:1906.05936* (2019).
- [77] Yue Yu, Jiaxiang Wu, and Junzhou Huang. 2019. Exploring Fast and Communication-Efficient Algorithms in Large-scale Distributed Networks. *arXiv e-prints*, Article arXiv:1901.08924 (Jan. 2019), arXiv:1901.08924 pages. arXiv:math.OA/1901.08924
- [78] Yue Yu, Jiaxiang Wu, and Longbo Huang. 2018. Double Quantization for Communication-Efficient Distributed Optimization. *arXiv e-prints*, Article arXiv:1805.10111 (May 2018), arXiv:1805.10111 pages. arXiv:math.OA/1805.10111
- [79] Binhang Yuan, Anastasios Kyrillidis, and Christopher M. Jermaine. 2019. Distributed Learning of Deep Neural Networks using Independent Subnet Training. *arXiv e-prints*, Article arXiv:1910.02120 (Oct. 2019), arXiv:1910.02120 pages. arXiv:cs.LG/1910.02120
- [80] Sergey Zagoruyko and Nikos Komodakis. 2016. Wide Residual Networks. *arXiv e-prints*, Article arXiv:1605.07146 (May 2016), arXiv:1605.07146 pages. arXiv:cs.CV/1605.07146
- [81] Matthew D Zeiler and Rob Fergus. 2013. Visualizing and Understanding Convolutional Networks. *arXiv e-prints*, Article arXiv:1311.2901 (Nov. 2013), arXiv:1311.2901 pages. arXiv:cs.CV/1311.2901
- [82] Jian Zhang, Christopher De Sa, Ioannis Mitliagkas, and Christopher Ré. 2016. Parallel SGD: When does averaging help? *arXiv e-prints*, Article arXiv:1606.07365 (June 2016), arXiv:1606.07365 pages. arXiv:stat.ML/1606.07365
- [83] Sixin Zhang, Anna E Choromanska, and Yann LeCun. 2015. Deep learning with elastic averaging SGD. In *Advances in neural information processing systems*. 685–693.
- [84] Wentao Zhu, Can Zhao, Wenqi Li, Holger Roth, Ziyue Xu, and Daguang Xu. 2020. LAMP: Large Deep Nets with Automated Model Parallelism for Image Segmentation. *arXiv e-prints*, Article arXiv:2006.12575 (June 2020), arXiv:2006.12575 pages. arXiv:cs.CV/2006.12575
- [85] Martin Zinkevich, Markus Weimer, Lihong Li, and Alex J Smola. 2010. Parallelized stochastic gradient descent. In *Advances in neural information processing systems*. 2595–2603.